PHYSICAL REVIEW VOLUME 131, NUMBER 2 15 JULY 1963

Effect of Impurities upon Critical Temperature of Anisotropic Superconductors*

DAVID MARKOWITZ† AND LEO P. KADANOFF
Physics Department, University of Illinois, Urbana, Illinois

(Received 7 March 1963)

The changes in critical temperature upon doping a superconductor are accounted for theoretically by solving a BCS-like model which includes anisotropy. This anisotropy is introduced via a factorable pairing potential $V_{pp'}=[1+a(\hat{\Omega})]V[1+a(\hat{\Omega}')]$ which depends on the momenta of the paired particles relative to the crystal axes. The impurities have two effects upon T_c: They gradually change the gross properties of the system and, hence, produce a linear change in T_c (valence effect), and in addition they abruptly reduce T_c by reducing the anisotropy of the energy gap (mean-free-path effect). By adjusting parameters representing the strengths of these effects, we have fit theory to experiments on Sn, In, and Al alloy systems. We find $\langle a^2\rangle\sim 0.01$, while "valence" parameters vary strongly with impurity and do not depend simply on valence. The major gap in the theory is in the unknown ratio of the mean collision times for smoothing out anisotropy and for transport.

I. INTRODUCTION

THIS paper aims to provide a quantitative understanding of the changes in critical temperature produced by doping a superconductor with small amounts of nonmagnetic impurities.[1–3] These changes may be summarized as follows. Initially there is a drop in T_c which is almost linear and depends primarily on the mean free path l. This behavior persists until l approaches[4] $\xi_0\approx\bar{v}_F/\pi\Delta(0)$, the superconducting coherence distance, corresponding usually to about 1% of impurity. Then the material enters a region where the further changes in T_c are determined by the specific impurity. These two regions have been called the "mean-free-path" region and the "valence" region. The latter is partially a misnomer since properties other than valence also operate. With this caution we shall accept the term "valence." The total change in T_c caused by doping which does not alter the crystal structure is always only a few percent. In Fig. 1 we display typical data for three different impurities in tin.

The simplest theoretical picture of these changes is obtained by applying the BCS formula[5]

$$kT_c=1.14\omega_D\exp[-1/VN(0)],\qquad(1)$$

and saying that impurities will change each of the parameters on the right-hand side and, hence, will modify T_c. However, a cursory examination of the problem will indicate that this cannot be a full explanation. We have said that the greatest change in T_c is only a few percent. This is evidence that the parameters in (1) themselves vary only by a few percent. Certainly in the lowest concentration region, e.g., in the free-path region, the variations should be sufficiently gentle to allow us to consider only the linear term in a power series expansion in impurity concentration. Then (1) tells us that T_c will likewise vary linearly with concentration. However, Fig. 1 is hardly the plot of a linear relation. Moreover, solely on the basis of this type of reasoning, it is impossible to find either a free-path effect or curvature around ξ_0.

In order to come closer to the truth, we must account in greater detail for the operations of the superconducting interaction in the presence of impurity scattering centers. Then we might expect that a property of the pairing in the pure material becomes diminished by scattering and that a characteristic free path is about the extension of a pair, ξ_0. Early attempts in this direction[6] grossly overestimated the reduction in T_c caused by impurities.There are two rather subtle pitfalls which must be avoided in order to prevent this overestimate. The first pitfall lies in the fact that the pairing in the presence of the impurities is no longer of states $(\mathbf{p}\uparrow)$, $(-\mathbf{p}\downarrow)$ but instead the pairing is between time-reversed exact eigenstates of the doped normal metal. This change in the nature of the pairing was pointed out independently by Anderson,[7] and Bardeen and Mattis.[8] The other pitfall is even more subtle. It turns out that the effect one is looking for is so small that the cutoff at ω_D has to be handled just right. BCS cut off their gap equation by limiting the pairs to be composed of particles with kinetic energies within ω_D of the Fermi energy; as we discuss below a more proper cutoff procedure limits the consideration to those particles whose total energy (kinetic plus po-

---

* This research was supported by the U. S. Army Research Office (Durham).

† Present address: Rutgers University, New Brunswick, New Jersey.

[1] E. A. Lynton, B. Serin, and M. Zucker, J. Phys. Chem. Solids **3**, 165 (1957); R. I. Gayley, Jr., E. A. Lynton, and B. Serin, Phys. Rev. **126**, 43 (1962).

[2] G. Chanin, E. A. Lynton, and B. Serin, Phys. Rev. **114**, 719 (1959).

[3] D. P. Seraphim, C. Chiou, and D. J. Quinn, Acta Met. **9**, 861 (1961). We thank Dr. Seraphim for informing us of his work.

[4] We use units in which $\hbar=1$. The bar in $\bar{v}_F$ denotes an average over the Fermi surface.

[5] J. Bardeen, L. N. Cooper, and J. R. Schrieffer, Phys. Rev. **108**, 1175 (1957).

[6] H. Suhl and B. T. Matthias, Phys. Rev. **114**, 977 (1959); K. Nakamura, Progr. Theoret. Phys. (Kyoto) **21**, 435 (1959); D. J. Kenworthy and D. ter Haar, Phys. Rev. **123**, 1181 (1961).

[7] P. W. Anderson, J. Phys. Chem. Solids **11**, 26 (1959).

[8] J. Bardeen and D. Mattis, Phys. Rev. **111**, 412 (1958).

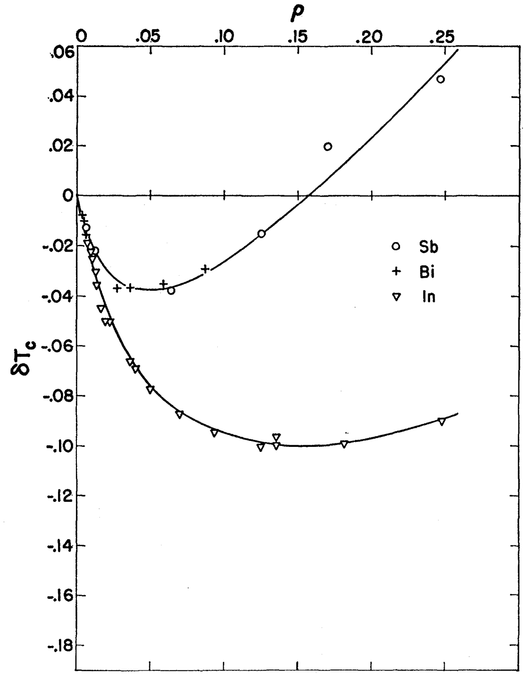

FIG. 1. δT_c versus ρ for three tin alloy systems, taken from Lynton *et al.* and from Seraphim *et al.* including data of Doidge. ρ, the residual resistivity ratio, is proportional to $1/l$. For small ρ there is a mean-free-path effect; for larger ρ, a "valence" effect. When $\rho = 0.05$, $l \approx \xi_0$.

tential) lies within ω_D of the Fermi energy. Anderson[7] recognized both of these pitfalls and proved a theorem which said that T_c is unaffected by the addition of impurities whenever the electron-electron interaction is assumed independent of particle momenta within a range about the Fermi surface. [Anderson claimed in this paper less than his theorem actually proved. His claim was that his result was valid for a "dirty" superconductor, one for which $\Delta(0)\tau \lesssim 1$, where τ is the mean time for scattering$= l/\bar{v}_F$. We shall demonstrate that there should be no restriction at all on τ.] This theorem serves to explain how the earlier calculations, which used a cutoff in the kinetic energy, could overestimate the effect of the impurities.

At this stage the problem was to find a likely feature of the pairing whose diminution could produce the curves in Fig. 1. On the basis of a variety of other experimental evidence,[9] Anderson decided that this property was anisotropy in the effective electron-electron interaction. The basic idea is that the internactio via phonons must depend upon the direction of electronic momenta relative to the crystal axes, and in the pure material the electrons take maximum advantage of this anisotropy in forming pairs. In the impure material scattering will act to smear the electronic states over the Fermi surface. The net effect will be to produce pairs which are less able to take advantage of anisotropy, thus, reducing the critical temperature. It is anticipated that when $l \sim \xi_0$, i.e., when a $(\mathbf{p}\uparrow)(-\mathbf{p}\downarrow)$ pair is broken up within the distance such a pair would ordinarily occupy, then a substantial fraction of the anisotropy will have been eliminated and the rate of reduction of T_c will level off. Hence, the curvature in Fig. 1. In the "dirty" region where $l < \xi_0$ the pairing is of states comprised almost equally of large portions of the Fermi surface and the anisotropy (or free path) effect is no longer the central effect.

Thus, our picture is that the change in T_c comes from two sources: (a) the reduction in anisotropy, and (b) all the changes in the gross parameters of the system. Included in (b) are the changes in the values of ω_D, V, and $N(0)$ of Eq. (1) plus the addition of such new events as the scattering of phonons by impurities. Included also in (b) would be any other effect excluded from (a). The point is that there is a complex pattern of changes comprising (b) whose net effect has been termed the "valence" effect and which can be approximated by a term linear in impurity concentration. Then this part of δT_c may be accounted for by a simple one-parameter fit of the data. However, in order to investigate the aptness of the entire picture, the anisotropy effect must be calculated in detail.

In the next section of this paper, we shall introduce a simple model to determine this effect as part of a description of the doped superconductor relevant to all temperatures. This model was proposed and solved by several other groups, in addition to ourselves, at roughly the same time.[10] The formulas of this section are essentially identical to those derived by the other groups. We present this section both for reasons of completeness and also because we believe that an alternative treatment might serve to further illuminate the basic ideas which underlie this rather subtle calculation. In Sec. III, the solution is specialized to the determination of T_c. The main new results of this paper are to be found in Sec. IV in which a detailed comparison of theory and experiment is presented. We evaluate results and draw conclusions in Sec. V.

II. THEORY

A general electron-electron interaction may be written as

$$H_{\text{int}} = \frac{1}{\text{vol}} \sum_{\mathbf{p}_1', \mathbf{p}_2', \mathbf{p}_1, \mathbf{p}_2, \sigma_1, \sigma_2} \langle \mathbf{p}_1'\mathbf{p}_2' | V | \mathbf{p}_1\mathbf{p}_2 \rangle \times \delta_{\mathbf{p}_1+\mathbf{p}_2, \mathbf{p}_1'+\mathbf{p}_2'} c_{\mathbf{p}_1'\sigma_1}{}^{\dagger} c_{\mathbf{p}_2'\sigma_2}{}^{\dagger} c_{\mathbf{p}_2\sigma_2} c_{\mathbf{p}_1\sigma_1}, \tag{2}$$

---

[9] N. E. Phillips, Phys. Rev. Letters **1**, 363 (1958) and H. A. Boorse, *ibid.* **2**, 391 (1959) on specific heat; P. L. Richards and M. Tinkham, *ibid.* **1**, 318 (1958) on optical absorption; L. C. Hebel and C. P. Slichter, Phys. Rev. **107**, 901 (1957) on nuclear spin relaxation. More recently, see R. W. Morse, T. Olsen, and J. D. Gavenda, Phys. Rev. Letters **3**, 15 (1959); **3**, 193(E) (1959) on ultrasonic attenuation; P. L. Richards, Phys. Rev. Letters **7**, 412 (1961) on optical absorption; and M. Yaqub, Cryogenics **1**, 166 (1961) on specific heat.

[10] T. Tsuneto, Progr. Theoret. Phys. (Kyoto) **28**, 857 (1962); C. Caroli, P. G. de Gennes and J. Matricon (to be published); D. Markowitz and L. P. Kadanoff, Bull. Am. Phys. Soc. **7**, 534 (1962). Work along similar lines has been done by L. Gruenberg (private communication).

where vol is the volume of the system. The part of this interaction responsible for superconductivity couples pairs of particles with opposite momenta, involving

$$V_{\mathbf{p}\mathbf{p}'}=-\langle \mathbf{p}',-\mathbf{p}'|V|\mathbf{p},-\mathbf{p}\rangle. \tag{3}$$

In order to have the simplest possible model which includes anisotropy, we choose the factorized form

$$V_{\mathbf{p}\mathbf{p}'}=[1+a(\hat{\Omega})]V[1+a(\hat{\Omega}')]. \tag{4}$$

Here, $\hat{\Omega}$ and $\hat{\Omega}'$ are unit vectors which point along the directions of $\mathbf{p}$ and $\mathbf{p}'$, respectively. The quantities $a(\hat{\Omega})$ describe the anisotropy of the interaction. They are chosen so that their average

$$\langle a\rangle=\int\frac{d\Omega}{4\pi}a(\hat{\Omega})=0.$$

In the absence of impurities, the BCS variational method can be extended to the case in which the pairing potential takes the form (4). The only material change from BCS is that the energy gap becomes a function of angle. Specifically, the angular dependence is $[1+a(\hat{\Omega})]$ at all temperatures. The experiments of Hebel,[11] Masuda,[12] and Masuda and Redfield[13] are explainable on the basis of such a temperature-independent gap anisotropy.

This evidence is offered not as proof of the correctness of our model, but simply as a rough confirmation of its reliability. It should be understood that the separability assumption is an *ad hoc* representation of complex physical effects. All of the anisotropy of the problem is lumped into $a(\hat{\Omega})$: anisotropy in the phonon spectrum, in the electron-phonon matrix element, in the electronic density of states. Furthermore, we must point out that we are assuming homogeneity in space. This means the following: The gap $\Delta(\hat{\Omega})$ depends on the direction of $\hat{\Omega}$ relative to the crystal axes. However, laboratory specimens are polycrystals. In each grain of a polycrystal the axes have a different orientation, i.e., $\hat{\Omega}$ is measured with respect to a different reference direction. Thus, the quantity $\Delta(\vec{X})$, where $\vec{X}$ is a vector in the laboratory, changes somewhat abruptly at a grain boundary. This implies: (1) There is a surface energy associated with grain boundaries, and (2) the wave function or propagator of a quasiparticle changes from grain to grain. Both of these circumstances are modified by the scattering of quasiparticles by impurities. This is principally what we are neglecting by assuming homogeneity in space. (We likewise neglect any other possibility for inhomogeneities, such as local variations in the gap caused by a strain field surrounding an impurity or by resonant scattering of electrons of the nature proposed for transition element impurities by Suhl *et al.*[14])

We return to our simple model.

As soon as impurities are introduced into the system, it becomes impossible to make direct use of the BCS procedure because one cannot find the single-particle states even in the normal metal. Fortunately, one neither wants nor needs these states. The only physical quantities are sums over all such states and in these sums the complexities of the individual states disappear. In order to make use of this simplification, we shall employ as our basic computational tool Green's functions, which are sums over all states of the products of creation and annihilation operators. These Green's functions are a standard computational tool in the analysis of doped normal[15] and superconducting[16,17] materials.

We consider for any Fermion system the function

$$G(\mathbf{p},t-t')=(1/i)\langle T[c_{\mathbf{p}\sigma}(t)c_{\mathbf{p}\sigma}{}^{\dagger}(t')]\rangle, \tag{5}$$

which is the average in the grand canonical ensemble of a propagator describing the impurity averaged[18] progress of a particle through the system. In a superconductor, we must consider an additional propagator

$$F^{\dagger}(\mathbf{p},t-t')=(1/i)\langle T[c_{-\mathbf{p}\downarrow}{}^{\dagger}(t)c_{\mathbf{p}\uparrow}{}^{\dagger}(t')]\rangle, \tag{6}$$

which describes the impurity average of a probability amplitude for pair formation. The single-particle states are defined by G, the pairing by F.

For every change in the single-particle states there is a corresponding change in the nature of the pairing.[7,8] If we are to satisfy Anderson's theorem, we must seek a computational scheme which handles G and F symmetrically.

Nambu[19] recognized a symmetry between G and F and established a simple and elegant formalism based upon it. He introduced the pseudospinor field

$$\psi_{\mathbf{p}}=\begin{pmatrix} c_{\mathbf{p}\uparrow} \\ c_{-\mathbf{p}\downarrow}{}^{\dagger}\end{pmatrix} \tag{7a}$$

and the Pauli spin matrices

$$\tau_1=\begin{pmatrix}0 & 1\\ 1 & 0\end{pmatrix},\quad \tau_3=\begin{pmatrix}1 & 0\\ 0 & -1\end{pmatrix}. \tag{7b}$$

---

[11] L. C. Hebel, Phys. Rev. **116**, 79 (1959).

[12] Y. Masuda, Phys. Rev. **126**, 1271 (1962).

[13] Y. Masuda and A. G. Redfield, Phys. Rev. **125**, 159 (1962).

[14] H. Suhl, D. R. Fredkin, J. S. Langer, and B. T. Matthias (to be published).

[15] J. Bardeen, in *Handbuch der Physik*, edited by S. Flügge (Springer-Verlag, Berlin, 1950), Vol. 15, p. 312; E. Abrahams and P. R. Weiss, Phys. Rev. **111**, 722 (1958); S. F. Edwards, Phil. Mag. **3**, 1020 (1958).

[16] A. A. Abrikosov and L. P. Gor'kov, Zh. Eksperim. i Teor. Fiz. **35**, 1558 (1958); **36**, 319 (1959) [translations: Soviet Phys.—JETP **8**, 1090 (1959); **9**, 220 (1959)].

[17] G. Rickayzen, in *The 1961 Bergen Lecture Notes on the Many-Body Problem*, edited by Christian Fronsdal (W. A. Benjamin, New York, 1962), p. 85.

[18] By "impurity averaged" we mean that randomization of impurity sites has been carried out in the same manner as in Ref. 14.

[19] Y. Nambu, Phys. Rev. **117**, 648 (1960).

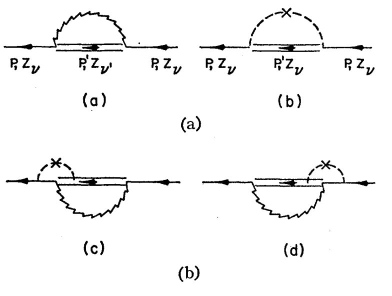

FIG. 2. Graphs used for calculating Σ. (a) electron-electron interaction via phonons; (b) second Born approximation to electron-impurity scattering; (c) and (d) renormalization of electron-electron interaction, estimated to be very small. The full Green's function is denoted by a double line.

He defined matrix Green's functions

$$g(\mathbf{p},t-t')=(1/i)\langle T[\psi_{\mathbf{p}}(t)\psi_{\mathbf{p}}^{\dagger}(t')]\rangle. \tag{8}$$

G and F are diagonal and off-diagonal components of g and are automatically dealt with symmetrically through the manipulations of g.

In the evaluation of $g(\mathbf{p},t-t')$ it is convenient to take t and t' to be pure imaginary times each of which lies in the interval $[0,-i\beta]$. The time ordering in (8) is then defined to be an ordering according to the relative magnitudes of it and it'. When g is defined in this way it is possible to prove[20] that g has the convenient Fourier series representation,

$$g(\mathbf{p},t-t')=\frac{1}{-i\beta}\sum_{\nu}\epsilon^{-iz_\nu(t-t')}g(\mathbf{p},z_\nu),$$
$$z_\nu=\pi\nu/-i\beta,\quad \nu=\text{odd integer}. \tag{9}$$

Using Nambu's Hamiltonian,[19] in the absence of interactions we have $g_0(\mathbf{p},z)=[z-\epsilon_p\tau_3]^{-1}$. To account for the workings of interactions we define a self-energy Σ according to

$$g(\mathbf{p},z)=[z-\epsilon_{\mathbf{p}}\tau_3-\Sigma(\mathbf{p},z)]^{-1}. \tag{10}$$

The advantage of the Nambu scheme lies in the fact that $\Sigma(\mathbf{p},z)$ may be expanded in almost the standard fashion in a power series in the interaction potentials and g. (See Ref. 20, Chap. V for a discussion of this perturbation theory for Σ.) For zero-range interactions the only difference from the usual case lies in the appearance of a factor τ_3 at each vertex. Even though the perturbation theory for G does not converge in a superconductor, this perturbation theory for the Nambu Σ appears to converge rapidly.

We consider two contributions to Σ depicted in Fig. 2. Figure 2(a) shows the interaction responsible for the superconducting transition. The relevant portion of this diagram is the part that represents the pair formation and destruction processes induced by the electron-electron interaction. This part is off diagonal in the representation in which τ_3 is diagonal. It is given by

$$\Sigma_s(\mathbf{p},z)=\left[-i\int\frac{d^3p'}{(2\pi)^3}V_{\mathbf{p}\mathbf{p}'}\tau_3 g(\mathbf{p}',t-t')\Big|_{t'=t}\tau_3\right]_{\text{o.d.}},$$

where o.d. stands for off diagonal. With the aid of (9) we can write this contribution as

$$\Sigma_s(\mathbf{p},z)=-i\frac{1}{-i\beta}\sum_{\nu'}\int\frac{d^3p'}{(2\pi)^3}V_{\mathbf{p}\mathbf{p}'}[\tau_3 g(\mathbf{p},z_{\nu'})\tau_3]_{\text{o.d.}}. \tag{11}$$

The momentum integral contributes only very near the surface of the Fermi sea. Therefore, we can write

$$\int\frac{d^3p'}{(2\pi)^3}=N(0)\int\frac{d\Omega'}{4\pi}\int d\epsilon', \tag{12}$$

where $\epsilon'=(p'^2/2m)-\mu$ is the kinetic energy measured from the surface of the Fermi sea, $\int d\Omega'/4\pi$ is a solid angle integral over the directions of $\mathbf{p}'$, and $N(0)=m\bar{p}_F/2\pi^2$ is the density of states at the Fermi surface. With this writing, (11) becomes

$$\Sigma_s(\epsilon,\hat{\Omega},z)=-i\frac{1}{-i\beta}\sum_{\nu}N(0)V\int\frac{d\Omega'}{4\pi}[1+a(\hat{\Omega})][1+a(\hat{\Omega}')]\times\int d\epsilon'[\tau_3 g(\epsilon,\hat{\Omega},z_{\nu'})\tau_3]_{\text{o.d.}}. \tag{13}$$

There is also a diagonal contribution from this graph proportional to τ_3. Since this represents simply a shift in the zero point of energies, almost identical in normal and superconducting phases, we shall not consider it here.

The other graph we consider is that shown in Fig. 2(b). It represents the scattering of an electron by a single impurity in the second Born approximation. (For random placement of impurities, the second-order term coming from scatterings off different impurities averages to zero because of the incoherence of these processes.) If the electron-impurity interaction is represented by the potential $v(|\mathbf{r}-\mathbf{R}|)$, this term in the self-energy can be written as

$$\Sigma_I(\mathbf{p},z)=n_I\int\frac{d^3p'}{(2\pi)^3}|v(\mathbf{p}-\mathbf{p}')|^2\tau_3 g(\mathbf{p}',z)\tau_3, \tag{14}$$

where n_I is the density of impurities and $v(\mathbf{p}-\mathbf{p}')$ the Fourier transform of $v(|\mathbf{r}-\mathbf{R}|)$. The diagonal terms in (14) represent the scattering of the quasiparticles by the impurities; the off-diagonal terms describe impurity-induced pair breakup and recombination processes.

Notice that in (14) $|v(\mathbf{p}-\mathbf{p}')|^2$ is proportional to the Born approximation for the differential scattering cross section. In fact, the relation is

$$\frac{d\sigma}{d\Omega'}(\mathbf{p}\rightarrow\mathbf{p}')=\frac{m^2}{4\pi^2}|v(\mathbf{p}-\mathbf{p}')|^2. \tag{15}$$

---

[20] L. P. Kadanoff and G. Baym, *Quantum Statistical Mechanics* (W. A. Benjamin, New York, 1962), p. 18–19.

We can improve our evaluation of the self-energy (14) by using the actual differential cross section in (14) instead of just the Born approximation. With this replacement, (14) becomes

$$\Sigma_I(\mathbf{p},z)=n_I\frac{4\pi^2}{m^2}\int\frac{d^3p'}{(2\pi)^3}\frac{d\sigma}{d\Omega'}(\mathbf{p}\rightarrow\mathbf{p}')\tau_3 g(\mathbf{p}',z)\tau_3. \tag{16}$$

We are interested in the situation in which the initial particle momentum lies very close to the Fermi surface. The final momentum must be close to the Fermi surface because the integral in (16) only contributes in this region. Hence, $d\sigma/d\Omega'$ may be considered to be evaluated for $\epsilon\approx\epsilon'\approx0$. We consider it to be only a function of the angle between $\hat{\Omega}$ and $\hat{\Omega}'$. Thus, we can write (16) as

$$\Sigma_I(\epsilon,\hat{\Omega},z)=n_I\frac{2\bar{p}_F}{m}\int\frac{d\Omega'}{4\pi}\frac{d\sigma}{d\Omega'}(\hat{\Omega}\rightarrow\hat{\Omega}')$$
$$\times\int d\epsilon'\tau_3 g(\epsilon',\hat{\Omega}',z)\tau_3. \tag{17}$$

There are additional graphs which are linear in the density of impurities, those indicated in Figs. 2(c) and 2(d). These vertex corrections cause a slight renormalization of the effective electron-electron interaction. They are sufficiently small so that the resulting change in V (of order $1/\bar{p}_F l$) can be considered to produce a linear change in T_c. Hence, these graphs can be considered to be included in the "valence effect."

The self-energy is given by the sum of (13) and (17). We wish to substitute this result into (10) and solve self-consistently for $g(\mathbf{p},z)$. In obtaining this solution, it is vital to notice that the self-energy is independent of the kinetic energy, ϵ. Furthermore, we guess that $\Sigma(\hat{\Omega},z)$ only has terms proportional to the unit matrix and to τ_1. We can represent this guess by writing

$$\Sigma(\mathbf{p},z)=[1-Z(\hat{\Omega},z)]z+Z(\hat{\Omega},z)\Delta(\hat{\Omega},z)\tau_1. \tag{18}$$

Hence,

$$g^{-1}(\mathbf{p},z)=Z(\hat{\Omega},z)z-Z(\hat{\Omega},z)\Delta(\hat{\Omega},z)\tau_1-\epsilon\tau_3, \tag{19}$$

so that

$$g(\mathbf{p},z)=\frac{1}{Z(\Omega,z)}\frac{z+\Delta(\hat{\Omega},z)\tau_1+[\epsilon/Z(\Omega,z)]\tau_3}{z^2-[\epsilon/Z(\Omega,z)]^2-[\Delta(\hat{\Omega},z)]^2}. \tag{20}$$

This choice is motivated by the well-known form of $g(\mathbf{p},z)$ for the isotropic undoped superconductor. In that case $Z\equiv1$ and

$$g(\mathbf{p},z)=\frac{z+\Delta\tau_1+\epsilon\tau_3}{z^2-\epsilon^2-\Delta^2}. \tag{20a}$$

Notice that the poles in $g(\mathbf{p},z)$ at $z=\pm(\epsilon^2+\Delta^2)^{1/2}$ occur at the quasiparticle energies of the BCS theory.

We can do the ϵ' integrals which appear in the self-energy quite directly. From (20)

$$\int_{-\infty}^{\infty}d\epsilon'\tau_3 g(\epsilon',\hat{\Omega},z)\tau_3$$
$$=\int_{-\infty}^{\infty}d\left[\frac{\epsilon'}{Z(\Omega,z)}\right]\frac{z-\Delta(\hat{\Omega},z)\tau_1+[\epsilon'/Z(\Omega,z)]\tau_3}{z^2-[\Delta(\hat{\Omega},z)]^2-[\epsilon'/Z(\Omega,z)]^2}$$
$$=-\pi\frac{z-\Delta(\hat{\Omega},z)\tau_1}{\{[\Delta(\hat{\Omega},z)]^2-z^2\}^{1/2}}. \tag{21}$$

The square root in (21) is defined with a branch cut along the real axis. As $z\rightarrow\infty$ in the upper half-plane, this reduces to iz; as $z\rightarrow\infty$ in the lower half-plane it reduces to $-iz$.

With the aid of (21), (13) and (17) become

$$\Sigma_s(\hat{\Omega},z)=VN(0)[1+a(\hat{\Omega})]\int\frac{d\Omega'}{4\pi}\frac{1}{-i\beta}\sum_{\nu'}\pi i[1+a(\hat{\Omega}')]$$
$$\times\left[\frac{z_{\nu'}-\Delta(\hat{\Omega}',z_{\nu'})\tau_1}{\{[\Delta(\hat{\Omega}',z_{\nu'})]^2-z_{\nu'}^2\}^{1/2}}\right]_{\text{o.d.}} \tag{22}$$

and

$$\Sigma_I(\hat{\Omega},z)=\frac{\bar{v}_F n_I}{2}\int d\Omega'\frac{d\sigma}{d\Omega'}(\hat{\Omega}\rightarrow\hat{\Omega}')\frac{z-\Delta(\hat{\Omega}',z)\tau_1}{\{[\Delta(\hat{\Omega}',z)]^2-z^2\}^{1/2}}. \tag{23}$$

Thus, we verify that $\Sigma(\hat{\Omega},z)$ has no τ_3 term.

Since we are projecting out the off-diagonal part, (22) is of the form

$$\Sigma_s(\hat{\Omega},z)=[1+a(\hat{\Omega})]\epsilon_0\tau_1 \tag{24}$$

with

$$\epsilon_0=VN(0)\int\frac{d\Omega'}{4\pi}[1+a(\hat{\Omega}')]\frac{\pi}{\beta}$$
$$\times\sum_{\nu'}\frac{\Delta(\hat{\Omega}',z_{\nu'})}{\{[\Delta(\hat{\Omega}',z_{\nu'})]^2-z_{\nu'}^2\}^{1/2}}. \tag{25}$$

The ν' summation in (25) may be converted into an integral by means of a well-known trick which depends upon the mathematical identity

$$\frac{1}{-i\beta}\sum_{\nu}h(z_\nu)=-\oint_C\frac{dz}{4\pi}\tanh(\tfrac{1}{2}\beta z)h(z). \tag{26}$$

In Eq. (26), $h(z)$ is any analytic function of z and the contour C encircles, in the negative sense, all the poles of $\tanh(\frac{1}{2}\beta z)$. (These poles lie at $z=z_\nu$.) The contour may then be distorted to enclose all the singularities of $h(z)$ in the positive sense. For the particular $h(z)$ in (25), the singularities are branch lines on the real axis. (For example, the square root is defined to change sign at the real axis for Δ real and $z^2>\Delta^2$.) Thus, (25) becomes

$$\epsilon_0=-\frac{i}{4}VN(0)\oint_{C'}dz'\tanh(\tfrac{1}{2}\beta z')\int\frac{d\Omega'}{4\pi}[1+a(\hat{\Omega}')]\times\frac{\Delta(\hat{\Omega}',z')}{\{[\Delta(\hat{\Omega}',z')]^2-z'^2\}^{1/2}},\quad(27)$$

where C' encircles the real axis in the positive sense. The discontinuity across the real axis is just $-2i$ times the imaginary part of the integrand for z' just above the real axis. Therefore, (27) becomes

$$\epsilon_0=-\tfrac{1}{2}VN(0)\int_{-\infty}^{\infty}d\omega\tanh(\tfrac{1}{2}\beta\omega)\int\frac{d\Omega'}{4\pi}[1+a(\hat{\Omega}')]\times\operatorname{Im}\frac{\Delta(\hat{\Omega}',z')}{\{[\Delta(\hat{\Omega}',z')]^2-z'^2\}^{1/2}}\bigg|_{z'=\omega+i\eta}.\quad(28)$$

If Δ is a constant as in BCS, the integral in (28) diverges for large energies. The remedy for this is apparent: We introduce the cutoff at energies $\pm\omega_D$ which makes BCS convergent. BCS applies the cutoff in the kinetic energy variable ϵ; we instead cut off the frequency (total energy) variable ω in (28). These two cutoff procedures are indistinguishable for the pure material, but a more fundamental theoretical viewpoint indicates that the cutoff in ω is preferable. This preference results from the circumstance that the effective electron-electron interaction is, in a more accurate theory, frequency-dependent rather than ϵ-dependent. For the doped material Anderson[7] has shown that a cutoff in the true eigenenergy, rather than in the unperturbed Bloch energy, is a key step toward the proof of his theorem.

Now we gather the threads of our argument. We substitute the contributions (23) and (24) to the self-energy into the left-hand side of (18). This produces

$$\begin{aligned}\Sigma(\hat{\Omega},z)&=\Sigma_I(\hat{\Omega},z)+\Sigma_s(\hat{\Omega},z)\\&=\frac{n_I\bar{v}_F}{2}\int d\Omega'\frac{d\sigma}{d\Omega'}(\hat{\Omega}\to\hat{\Omega}')\frac{z-\Delta(\hat{\Omega}',z)\tau_1}{\{[\Delta(\hat{\Omega}',z)]^2-z^2\}^{1/2}}+[1+a(\hat{\Omega})]\epsilon_0\tau_1\\&=z[1-Z(\hat{\Omega},z)]+\Delta(\hat{\Omega},z)Z(\hat{\Omega},z)\tau_1.\end{aligned}\quad(29)$$

This equation splits into two components; the one proportional to τ_1 is

$$Z(\hat{\Omega},z)\Delta(\hat{\Omega},z)=\frac{n_I\bar{v}_F}{2}\int d\Omega'\frac{d\sigma}{d\Omega'}(\hat{\Omega}\to\hat{\Omega}')\frac{\Delta(\hat{\Omega}',z)}{\{[\Delta(\hat{\Omega}',z)]^2-z^2\}^{1/2}}+[1+a(\hat{\Omega})]\epsilon_0,\quad(30)$$

while the one proportional to the unit matrix is

$$Z(\hat{\Omega},z)=1+\frac{n_I\bar{v}_F}{2}\int d\Omega'\frac{d\sigma}{d\Omega'}(\hat{\Omega}\to\hat{\Omega}')\times\frac{1}{\{[\Delta(\hat{\Omega}',z)]^2-z^2\}^{1/2}}.\quad(31)$$

Finally, (31) may be used to eliminate $Z(\hat{\Omega},z)$ from (30), yielding

$$\Delta(\hat{\Omega},z)=\frac{n_I\bar{v}_F}{2}\int d\Omega'\frac{d\sigma}{d\Omega'}(\hat{\Omega}\to\hat{\Omega}')\frac{\Delta(\hat{\Omega}',z)-\Delta(\hat{\Omega},z)}{\{[\Delta(\hat{\Omega}',z)]^2-z^2\}^{1/2}}+[1+a(\hat{\Omega})]\epsilon_0.\quad(32)$$

Equation (32) is to be solved simultaneously with the cutoff version of (28)

$$\epsilon_0=-\tfrac{1}{2}VN(0)\int_{-\omega_D}^{\omega_D}d\omega\tanh(\tfrac{1}{2}\beta\omega)\int\frac{d\Omega'}{4\pi}[1+a(\hat{\Omega}')]\times\operatorname{Im}\frac{\Delta(\hat{\Omega}',z')}{\{[\Delta(\hat{\Omega}',z')]^2-z'^2\}^{1/2}}\bigg|_{z'=\omega+i\eta}.\quad(33)$$

In the absence of anisotropy ($a(\hat{\Omega})=0$), (32) implies $\Delta(\hat{\Omega},z)=\epsilon_0$. Hence, (33) becomes

$$1=VN(0)\int_{-\omega_D}^{\omega_D}\frac{d\omega}{2}\tanh(\tfrac{1}{2}\beta\omega)\operatorname{Re}\left[\frac{1}{(\omega^2-\epsilon_0^2)^{1/2}}\right].\quad(34)$$

Notice that, in accordance with Anderson's theorem, ϵ_0 is independent of impurity scattering in the isotropic case. The fact that ϵ_0 is the physical gap follows from specializing (20a) to the case $\Delta(\hat{\Omega},z)=\epsilon_0$ and $\epsilon=0$. Then $g(\mathbf{p},z)=[1/Z(z)][z+\epsilon_0\tau_1]/[z^2-\epsilon_0^2]$. The lowest singularity in $g(\mathbf{p},z)$ lies at $z=\pm\epsilon_0$; hence, the lowest quasiparticle energy is ϵ_0. We may cast Eq. (34) into BCS language. If we use $\epsilon=(\omega^2-\epsilon_0^2)^{1/2}$ as our integration variable, then (34) becomes

$$1=VN(0)\int_{-\omega_D'}^{\omega_D'}\frac{d\epsilon}{2E}\tanh(\tfrac{1}{2}\beta E),$$

where $E=(\epsilon^2+\epsilon_0^2)^{1/2}$ and $\omega_{D'}=(\omega_D^2-\epsilon_0^2)^{1/2}$. If $\omega_{D'}$ is taken independent of temperature, this is the standard BCS gap equation.

III. SPECIALIZATION TO CRITICAL TEMPERATURE

Instead of discussing (32) and (33) in their full generality, we now specialize to the case in which the temperature lies infinitesimally below T_c. In this case $\Delta(\hat{\Omega},z)$ is infinitesimal and may be neglected in all the denominators. Hence, (33) becomes

$$\epsilon_0=VN(0)\int_{-\omega_D}^{\omega_D}dz'\int\frac{d\Omega'}{4\pi}\tanh(\tfrac{1}{2}\beta_c z')\times\frac{1+a(\hat{\Omega}')}{2z'}\operatorname{Re}\Delta(\hat{\Omega}',z')\quad(35)$$

and (32) is

$$\Delta(\hat{\Omega},z)=-\frac{i}{z}\,\mathrm{sgn}[\mathrm{Im}(z)]\frac{n_I\bar{v}_F}{2}\int d\Omega'\frac{d\sigma}{d\Omega'}(\hat{\Omega}\rightarrow\hat{\Omega}')\times[\Delta(\hat{\Omega}',z)-\Delta(\hat{\Omega},z)]+[1+a(\hat{\Omega})]\epsilon_0, \tag{36}$$

where

$$\mathrm{sgn}(x)=\begin{cases}1 \text{ if } x>0\\ -1 \text{ if } x<0.\end{cases}$$

We cannot obtain an exact solution of (36) for a general form of the differential cross section because we cannot find the angular dependence of $\Delta(\hat{\Omega},z)$. However, for the special case in which the impurity scattering is isotropic (that is, pure S-wave scattering), we can solve (36) precisely for in this case $d\sigma/d\Omega'=\sigma/4\pi$ implies

$$\Delta(\hat{\Omega},z)=\Delta_0(z)+a(\hat{\Omega})\Delta_1(z). \tag{37}$$

We shall assume that (37) represents the angular dependence of $\Delta(\hat{\Omega},z)$ even when the scattering is not isotropic. In other words, our assumptions is that impurity scattering changes the degree of anisotropy through Δ_1 but not the anisotropy function itself $a(\hat{\Omega})$.

We determine the two coefficients, Δ_0 and Δ_1, by taking the angular average of Eq. (36) and by taking the angular average of $a(\hat{\Omega})$ times Eq. (36). Thus, we find

$$\Delta_0(z)=\epsilon_0 \tag{38}$$

and

$$\int\frac{d\Omega}{4\pi}[a(\hat{\Omega})]^2\Delta_1(z)=-\frac{i}{z}\,\mathrm{sgn}[\mathrm{Im}(z)]\frac{n_I\bar{v}_F}{2}\int d\Omega'\int\frac{d\Omega}{4\pi}\times\{a(\hat{\Omega})a(\hat{\Omega}')-[a(\hat{\Omega})]^2\}\frac{d\sigma}{d\Omega'}(\hat{\Omega}\rightarrow\hat{\Omega}')+\int\frac{d\Omega}{4\pi}[a(\hat{\Omega})]^2\epsilon_0. \tag{39}$$

We write the angular average of $[a(\hat{\Omega})]^2$ as $\langle a^2\rangle$. Because $d\sigma/d\Omega'$ $(\hat{\Omega}\rightarrow\hat{\Omega}')$ depends only on the angle between $\hat{\Omega}$ and $\hat{\Omega}'$,

$$\int d\Omega'\int\frac{d\Omega}{4\pi}[a(\hat{\Omega})]^2\frac{d\sigma}{d\Omega'}(\hat{\Omega}\rightarrow\hat{\Omega}')=\langle a^2\rangle\int d\Omega'\int\frac{d\Omega}{4\pi}\frac{d\sigma}{d\Omega'}(\hat{\Omega}\rightarrow\hat{\Omega}').$$

Hence, (39) may also be written as

$$\left\{1-\frac{i\,\mathrm{sgn}[\mathrm{Im}(z)]}{2z\tau_a}\right\}\Delta_1(z)=\epsilon_0 \tag{40}$$

with

$$\frac{1}{\tau_a}=n_I\bar{v}_F\int d\Omega'\int\frac{d\Omega}{4\pi}\frac{d\sigma}{d\Omega'}(\hat{\Omega}\rightarrow\hat{\Omega}')\left[1-\frac{a(\hat{\Omega})a(\hat{\Omega}')}{\langle a^2\rangle}\right]. \tag{41}$$

Notice that τ_a may be interpreted as a collision time which describes the mean time for the smoothing out of an anisotropic distribution proportional to $1+a(\hat{\Omega})$.

From (37), (38), and (40),

$$\Delta(\hat{\Omega},z)=\epsilon_0+\frac{\epsilon_0 a(\hat{\Omega})}{1-\{i\,\mathrm{sgn}[\mathrm{Im}(z)]/2z\tau_a\}} \tag{42}$$

so that Eq. (35) for the critical temperature becomes

$$\epsilon_0=VN(0)\int_0^{\omega_D}\frac{d\omega}{\omega}\int\frac{d\Omega'}{4\pi}[1+a(\hat{\Omega}')]\tanh(\tfrac{1}{2}\beta_c\omega)\times\mathrm{Re}\left[1+\frac{a(\hat{\Omega}')}{1-\{i\,\mathrm{sgn}[\mathrm{Im}(z)]/2z\tau_a\}}\right]_{z=\omega+i\eta}\epsilon_0$$

or

$$1=VN(0)\int_0^{\omega_D}\frac{d\omega}{\omega}\tanh(\tfrac{1}{2}\beta_c\omega)\left[1+\frac{\langle a^2\rangle}{1+(2\omega\tau_a)^{-2}}\right]. \tag{43}$$

In the absence of impurities, $\tau_a=\infty$, (43) reduces to the usual BCS formula with an effective interaction $V_{\mathrm{eff}}=V[1+\langle a^2\rangle]$. Therefore, following the BCS weak-coupling solution,

$$kT_c=1.14\omega_D\exp\{-[VN(0)(1+\langle a^2\rangle)]^{-1}\}\,;\ \tau_a=\infty. \tag{44a}$$

When there are so many impurities present that $\omega_D\tau_a\ll1$, the term proportional to $\langle a^2\rangle$ in (38) becomes negligible so that we again reduce to BCS with $V_{\mathrm{eff}}=V$:

$$kT_c=1.14\omega_D\exp[-1/VN(0)];\quad \omega_D\tau_a\ll1. \tag{44b}$$

As τ_a decreases from ∞, kT_c progresses from a maximum given by (44a) to a minimum given by (44b). The experimentally interesting case is the one in which $\langle a^2\rangle\ll1$. In this case, the maximum relative change in T_c from the anisotropy effect is

$$\left(\frac{\delta T_c}{T_c}\right)_{\max}=\frac{T_c(\tau_a=0)-T_c(\tau_a=\infty)}{T_c}=-\frac{1}{VN(0)}\langle a^2\rangle.$$

Since $[1/VN(0)]\approx4$ for typical weak-coupling superconductors and $\langle a^2\rangle\approx0.01$ (as we shall see below), the maximum reduction in T_c which can come from this anisotropy effect ≈ 4%.

The T_c determined from (43) may be expanded in a power series in $\langle a^2\rangle$ whenever $\langle a^2\rangle\ll1$. This gives

$$\frac{\delta T_c(\tau_a)}{T_c}=-\langle a^2\rangle\int_0^{\omega_D}\frac{d\omega}{\omega}\frac{\tanh(\tfrac{1}{2}\beta_c\omega)}{1+(2\tau_a\omega)^2}, \tag{45}$$

where $\delta T_c(\tau_a)$ is the change in T_c relative to the value for a pure specimen, i.e., $\delta T_c(\infty)=0$. In writing (45) we have set $\tanh(\tfrac{1}{2}\beta_c\omega_D)=1$, which is perfectly allowable for a weak-coupling superconductor. It is con-

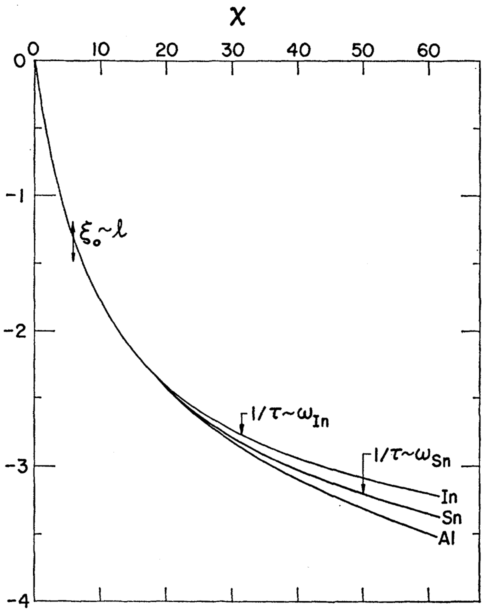

FIG. 3. I_c versus χ for In, Sn, and Al. $I_c \equiv \delta T_c [T_c \langle a^2 \rangle]^{-1}$; $\chi \equiv (kT_c\tau_a)^{-1}$.

venient for us to rewrite (45) in terms of the dimensionless variables

$$I_c = \delta T_c / [T_c \langle a^2 \rangle], \quad \chi = (kT_c\tau_a)^{-1}. \tag{46}$$

Notice that χ is proportional to the density of impurities. With these new variables, (45) becomes

$$I_c(\chi) = \int_0^{2\beta_c\omega_D/\chi} \frac{dy}{y} \frac{\tanh(\frac{1}{4}\chi y)}{1+y^2}. \tag{47}$$

Figure 3 displays the resulting curves for $I_c(\chi)$: the lowest for a fictitious metal with $\beta_c\omega_D = \infty$; the middle for Sn$(\beta_c\omega_D = 52)$; the highest for In$(\beta_c\omega_D = 32)$. Since Al has $\beta_c\omega_D = 320$, its curve is identical with the fictitious metal in the region plotted. For small χ, $I_c(\chi) \approx -(\pi/8)\chi$; for $10 \ll \chi \ll \beta\omega_D$, $I_c(\chi) \approx -\ln(0.5\chi)$. The differences between the various metals are slight.

Before we close this section, we indicate briefly the changes which would result from using a more realistic density-of-states function

$$N(0,\hat{\Omega}) = N(0)[1 + b(\hat{\Omega})],$$

where 0 refers to the Fermi surface. We choose $\langle b \rangle = 0$. It is easy to see that the modification in Eqs. (35) and (36) is simply to insert a factor $[1 + b(\hat{\Omega}')]$ into the integrand. Then each successive step following (36) may be retraced with slightly more care for the algebra. Our main interest is in the equation for T_c to replace (43). We might expect that the new expression in the brackets in (43) would look like

$$\left[1 + \frac{\langle a^2 \rangle + \langle ab \rangle}{1 + (2\omega\tau_a)^{-2}}\right].$$

Contrary to our expectation, we again obtain (43) providing that V is replaced by $V[1 + 2\langle ab \rangle]$. τ_a is again given by Eq. (41). The actual correction terms in (41) and (43) are not of order $\langle ab \rangle$ but of order $\langle a^2 b \rangle$. If b is the size of a, then $\langle a^2 b \rangle$ is at most $\sim \langle a^2 \rangle^{3/2}$ and probably much smaller. Thus, we are quite justified in considering an isotropic $N(0)$.

IV. COMPARISON WITH EXPERIMENT

In order to compare our results with experiment, we must follow the directions we set for ourselves in the Introduction. There we divided the change in T_c with doping into two parts. Part (a), the anisotropy effect, we have calculated in detail. Part (b), all the other effects, we have decided to fit to a single parameter (call it K^i) representing the coefficient of a term linear in impurity density. Thus, we expect

$$\delta T_c(\chi) = K^i \chi + \langle a^2 \rangle T_c I_c(\chi). \tag{48}$$

The numerical value of K^i depends in detail on both the impurity (denoted by i) and the host. On the other hand, the second term (anisotropy effect) in (48) depends only upon the mean free time τ_a and the properties of the host, $\langle a^2 \rangle$, T_c and weakly upon ω_D.

It is instructive to compare our theoretical result (48) with an empirical formula proposed by Seraphim *et al.*,[3] namely,

$$\delta T_c(\chi) = K_1^i \chi + K_2^i \chi \ln\chi. \tag{49}$$

[Actually Seraphim *et al.* wrote Eq. (49) in terms of the concentrations instead of the inverse mean free time but, since these are proportional, this difference is irrelevant.] The best way of comparing theory in Eq. (48) with the empiricism in (49) is to plot our result for I_c/χ against χ, with χ on a logarithmic scale. According to (49) this plot should yield a straight line. Figure 4 is such a plot. Notice that over two decades of χ this plot closely approximates a straight line. This

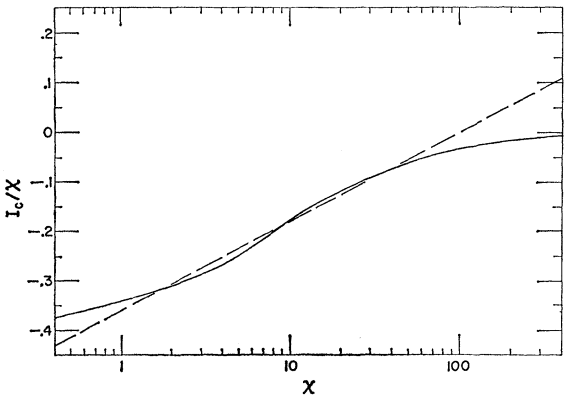

FIG. 4. I_c/χ versus χ for any system. In the interval $1 < \chi < 100$, the theoretical curve is approximated by the empirical rule $I_c = A\chi + B\chi \ln\chi$ proposed by Seraphim, Chiou, and Quinn.

serves as a rather impressive check of our theory. By using the straight-line fit in Fig. 4, we see that the theoretical result of Eq. (48) may approximately be replaced by

$$\begin{aligned}\delta T_c(\chi)&=K^i\chi+\langle a^2\rangle T_c(0.078)\chi\ln(\chi/100)\\&=[K^i-0.36\langle a^2\rangle T_c]\chi+0.078\langle a^2\rangle T_c\chi\ln\chi\\&\qquad\text{for}\quad 1<\chi<100.\end{aligned}\tag{50}$$

Consequently, the theory predicts that the coefficient $K_2{}^i$ in the empirical relation (49) should be dependent only upon the properties of the host and independent of the impurity. Thus, call this coefficient K_2.

Furthermore the theory, when put into the form (50), allows detailed comparison with experimental data if the coefficients $K_1{}^i$ and K_2 are obtainable from the data. Thus, we have an expectation of predicting numerical values for the anisotropy parameter of the host $\langle a^2\rangle$, and for the "valence effect" coefficient of the system of host and impurity K^i.

Unfortunately, expectation rather exceeds the state of our knowledge of real alloys. The difficulty begins with the realization that χ is not directly an experimental quantity. Instead, the experimenter determines ρ, the residual resistivity, or more precisely the ratio of the residual resistivity to the room-temperature (phonon-limited) resistivity. Since both χ and ρ are proportional to impurity density, they are proportional to one another; however, we do not know the constant of proportionality relating them. In other words, setting

$$\chi=\alpha^i\rho,\tag{51}$$

we can transform (49) or (50) into

$$\delta T_c(\rho)=c_1{}^i\rho+c_2{}^i\rho\ln\rho,\tag{52}$$

where again all quantities affected by the specific impurity are denoted by i. Our task is to obtain values of the K^i's from experimental determinations of the c^i's. In order to do this, we need α^i, a quantity we do not know.

To isolate the source of our ignorance, let us attempt to relate both ρ and χ to the same quantity, a mean collision time τ. First, we make use of Table I of Chanin *et al.*[2] (compiled from several sources listed therein) which gives the numerical factor relating ρ and $1/l$; say, $\rho=b/l$, where b is a known number depending on the host. Since $l=\bar{v}_F\tau_{\text{tr}}$, we have

$$\rho=b/(\bar{v}_F\tau_{\text{tr}}),\tag{53}$$

where τ_{tr} is the mean collision time for transport, and where $\bar{v}_F$ is the average value of the Fermi velocity and is also a known number for each host. (Actually, we have not used tabulated values of $\bar{v}_F$ but have calculated these values from formulas of Faber and Pippard[21] and from data obtained by these authors and by Faber.[22]) In this way, ρ can be related to $1/\tau_{\text{tr}}$ by a known number which is a property of the host. In addition we are able, through the definition of χ as $(kT_c\tau_a)^{-1}$ in (46), to relate χ to $1/\tau_a$, also by a known number which is a property of the host.

The collision time for transport τ_{tr} is given by the conventional theory as

$$\frac{1}{\tau_{\text{tr}}}=n_I\bar{v}_F\int\frac{d\Omega}{4\pi}\int d\Omega'\frac{d\sigma^i}{d\Omega'}(\hat{\Omega}\to\hat{\Omega}')[1-\hat{\Omega}\cdot\hat{\Omega}'],\tag{54}$$

where now the differential cross section is explicitly labeled i. Equation (41) tells us that

$$\frac{1}{\tau_a}=n_I\bar{v}_F\int\frac{d\Omega}{4\pi}\int d\Omega'\frac{d\sigma^i}{d\Omega'}(\hat{\Omega}\to\hat{\Omega}')\left[1-\frac{a(\hat{\Omega})a(\hat{\Omega}')}{\langle a^2\rangle}\right].\tag{41}$$

The angular dependence of neither $a(\hat{\Omega})$ nor $d\sigma^i/d\Omega'$ is known. Thus, the gap in our knowledge of α^i in (51) has been traced to the unknown ratio of (41) to (54),

$$\lambda^i=\frac{\tau_{\text{tr}}}{\tau_a}=\frac{\displaystyle\int\frac{d\Omega}{4\pi}\int d\Omega'\frac{d\sigma^i}{d\Omega'}(\hat{\Omega}\to\hat{\Omega}')\left[1-\frac{a(\hat{\Omega})a(\hat{\Omega}')}{\langle a^2\rangle}\right]}{\displaystyle\int\frac{d\Omega}{4\pi}\int d\Omega'\frac{d\sigma^i}{d\Omega'}(\hat{\Omega}\to\hat{\Omega}')[1-\hat{\Omega}\cdot\hat{\Omega}']}.\tag{55}$$

In other words, from

$$\chi=\lambda^i/(kT_c\tau_{\text{tr}})=\lambda^i[\bar{v}_F/(bkT_c)]\rho,\tag{56}$$

we can determine χ/λ^i from data on ρ—but not χ itself. Table I gives the values of b, $\bar{v}_F$, and the consequent values of $\chi/\lambda^i\rho$ used in our subsequent evaluations.

TABLE I. Values of b, $\bar{v}_F$, $\chi/(\lambda^i\rho)$, and $a\xi_0/0.15$.

	Sn	In	Al
$b=l\rho$(cm)	1.03×10^{-6}	1.15×10^{-6}	1.61×10^{-6}
$\bar{v}_F$(cm/sec)	6.84×10^{7}	7.20×10^{7}	1.25×10^{8}
$\chi/(\lambda^i\rho)$	135	140	500
$a\xi_0/0.15$(cm)	0.21×10^{-4}	0.24×10^{-4}	1.2×10^{-4}

In order to make further progress, we are forced to guess the value of λ^i. The existence of a mean-free-path effect, the very circumstance which stimulated this research, suggests that all λ^i for the same host have nearly the same value. Moreover, this value is likely to be about unity. In fact, if the impurity scattering is isotropic,

$$(d\sigma^i/d\Omega')(\hat{\Omega}\to\hat{\Omega}')=\sigma^i/4\pi,$$

then λ^i is exactly unity. In this way we are led to guess $\lambda^i=1$. This guess is the weak point in all our further analysis.

---

[21] T. E. Faber and A. B. Pippard, Proc. Roy. Soc. (London) **A231**, 336 (1955).

[22] T. E. Faber, Proc. Roy. Soc. (London) **A241**, 531 (1957).

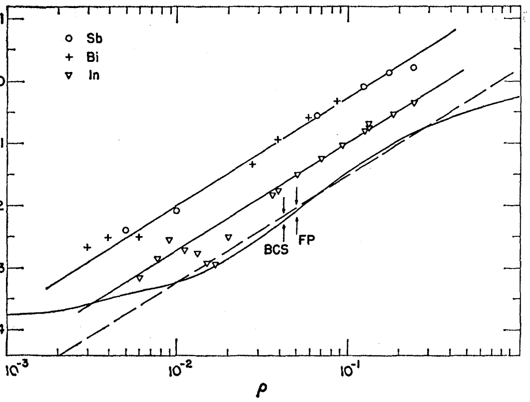

FIG. 5. $\delta T_c/\rho$ versus ρ for three tin alloy systems, taken from Fig. 1. Theoretical curve is taken from Fig. 4. The slope measures the strength of the anisotropy effect; the vertical distances between experimental and theoretical lines measure the "valence" effects. The arrows mark the approximate point at which the coherence distance equals the mean free path.

It is now profitable to follow the suggestion of Eq. (52) and graph experimental values of $\delta T_c/\rho$ versus ρ on a semilog plot. The assumption $\lambda^i=\text{const}$ has transformed our former prediction that $K_2^i=\text{const}$ in (49) into a prediction that $c_2^i=\text{const}$ in (52). Thus, we anticipate that the proposed graph will be a series of approximately parallel almost straight lines, each line pertaining to a different impurity in the same host. If the lines are truly parallel, then λ^i is truly a constant (not necessarily unity) to within experimental error.

Figure 5 is an example of the proposed graph for three different impurities in tin. (This graph is simply a replot of Fig. 1 on the new scale.) Within experimental error, the points for Bi and Sb fall on the same line and the points for In indeed fall on a parallel line. This confirmation of our prediction and of the assumption upon which it relies is striking.

In this figure we have added a theoretical curve for the change in T_c due to anisotropy, $\langle a^2\rangle T_c I_c'(\rho)$. (This curve is the one in Fig. 4 replotted in the new variables.) By adjusting $\langle a^2\rangle$ to be 0.019, we arrange to have the theoretical curve parallel to the experimental curves. Then by rewriting (48) as

$$\frac{\delta T_c}{\rho}=\left(\frac{\partial T_c}{\partial \rho}\right)_0^i+\langle a^2\rangle T_c\frac{I'_c(\rho)}{\rho}, \tag{57}$$

where $(\partial T_c/\partial\rho)_0^i$ contains all the effects other than anisotropy, we can obtain $(\partial T_c/\partial\rho)_0^i$ for each impurity. In this way we use the experimental data to determine one parameter for the host $\langle a^2\rangle$, and one parameter for each impurity $(\partial T_c/\partial\rho)_0^i$.

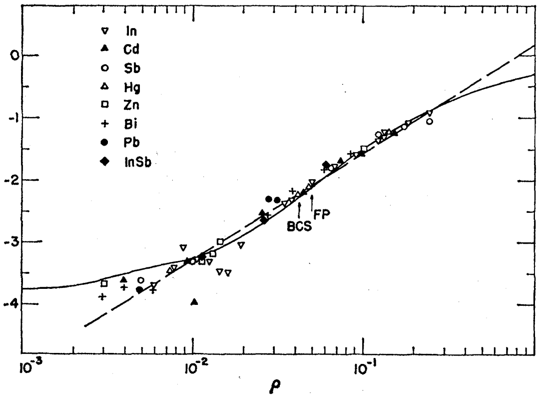

FIG. 6. $\delta T_c/\rho-(\partial T_c/\partial\rho)_0^i$ for all data on tin alloy systems known to the authors. The graph shows the reliability of the theoretical model as well as of the assumption $\lambda^i=\text{constant}$ for tin. The arrows mark the approximate point at which the coherence distance equals the mean free path.

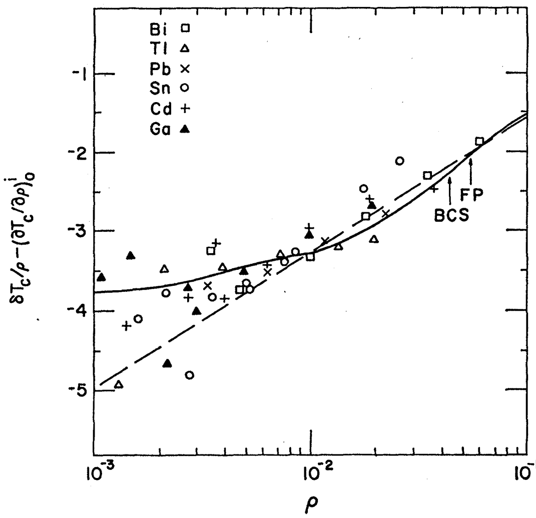

FIG. 7. $\delta T_c/\rho-(\partial T_c/\partial\rho)_0^i$ for data on In alloy systems, taken from Chanin, *et al.* Different values of λ^i would improve the fit for particular impurities. Notice that most data lie below the region fitted by the empirical rule of Seraphim *et al.* Compare the spread in data to that in Fig. 6. In-Ga is an anomalous system.

To fully exploit this procedure, we subtract $(\partial T_c/\partial\rho)_0^i$ from the experimental values of $\delta T_c/\rho$. This gives us an experimental determination of the anisotropy effect on T_c. It is expected to be independent of impurity. Figure 6 is such a plot for impurities in tin. In this figure we have included not only the data for Bi, Sb, and In, but essentially all the known data for a total of eight impurities (and hence nine adjustable parameters) in tin. The values of $(\partial T_c/\partial\rho)_0^i$ for the tin alloys are listed in Table II.

In Figs. 7, 8, and 9 we continue the comparison for indium and aluminum alloy systems. The values of parameters used to fit the data for these systems are listed in Tables III and IV. Finally, in Fig. 10 the experimental curves of Fig. 1 are again displayed, this time resolved into their anisotropy and "valence" parts.

There remains one last point to be explained. In Figs. 5 through 9 the position of the point $l=\xi_0$ has

TABLE II. Parameters for tin alloy systems under assumption $\lambda=1$. δz^i is the valence difference between impurity and host for free ions. ρ_I/n_I is the ratio of ρ to percent of impurity. The room-temperature resistivity for Sn is 13×10^{-6} Ω-cm. $\langle a^2\rangle$ for Sn=0.019.

Impurity	δz^i	$(\partial T_c/\partial\rho)_0^i$	ρ_I/n_I
In	−1	0.53	0.058
Cd	−2	0.68	0.14
Hg	−2	0.68	0.10[a]
Zn	−2	0.80	0.03[a]
InSb	0	0.93	0.060
Sb	+1	1.24	0.059
Bi	+1	1.24	0.085
Pb	0	1.45	0.043

[a] Denotes unusually large spread in data.

been indicated. It is obtained from the definition of χ for $\lambda^i=1$,

$$\chi=(kT_c\tau)^{-1}=\bar{v}_F/(kT_c l),$$

in conjunction with the BCS relation, $kT_c=a\bar{v}_F/\xi_0$. That is, from $\chi=(1/a)(\xi_0/l)$ and Eq. (56), one can locate the point $l=\xi_0$ on any of our graphs if one is told the value of a. Faber and Pippard[21] determine an experimental value of $a=0.15$ for Sn and Al. The BCS theory finds $a=0.18$ for all weak-coupling superconductors. The difference between the points $l=\xi_0$ due to

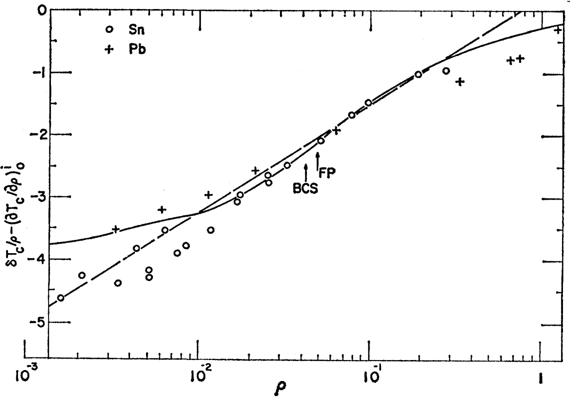

FIG. 8. $\delta T_c/\rho-(\partial T_c/\partial\rho)_0^i$ for Sn and Pb in In, taken from Fig. 7 and from Seraphim *et al.*, including data of Meissner *et al.* In-Sn fits a value of $\lambda\langle a^2\rangle=0.021$, while In-Pb fits a slightly smaller value.

TABLE III. Parameters for indium alloy systems under assumption $\lambda^i=\lambda=1$. δz^i is the valence difference between impurity and host for free ions. ρ_I/n_I is the ratio of ρ to percent of impurity. The room-temperature resistivity for In is 8.4×10^{-6} Ω-cm. $\langle a^2\rangle$ for In=0.021. (*Note.* Values in parentheses used to achieve fit in Fig. 8. In-Ga is an anomalous system.)

Impurity	δz^i	$(\partial T_c/\partial\rho)_0^i$	ρ_I/n_I
Cd	−1	1.00	0.041
Tl	0	1.84	0.026
Bi	+2	1.92	0.24
Pb	+1	2.08(1.92)	0.078
Sn	+1	2.08(2.56)	0.049
Ga	0	4.40	0.021

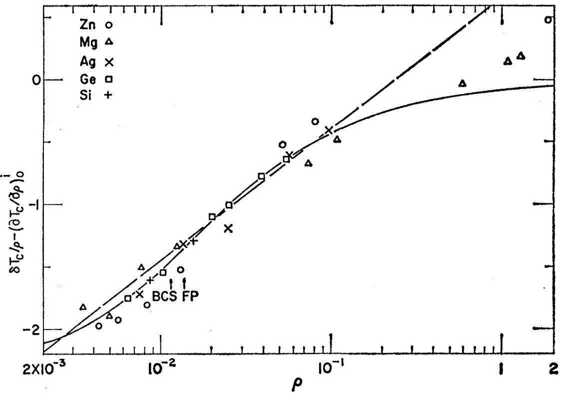

FIG. 9. $\delta T_c/\rho-(\partial T_c/\partial\rho)_0^i$ for data on Al alloy systems, taken from Chanin *et al.* and from Seraphim *et al.* As in the case of In, different values of λ^i would improve the fit for several impurities. Notice that most data lie above the mean-free-path region.

TABLE IV. Parameters for aluminum alloy systems under assumption $\lambda^i=\lambda=1$. δz^i is the valence difference between impurity and host for free ions. ρ_I/n_I is the ratio of ρ to percent of impurity. The room-temperature resistivity for Al is 2.7×10^{-6} Ω-cm. $\langle a^2\rangle$ for Al=0.011. (*Note.* * denotes unusually large spread in data.)

Impurity	δz^i	$(\partial T_c/\partial\rho)_0^i$	ρ_I/n_I
Zn	−1	−0.28	0.14*
Ag	−2	−0.22	0.52
Mg	−1	0.00	0.09*
Ge	+1	0.60	0.43
Si	+1	0.70	0.31

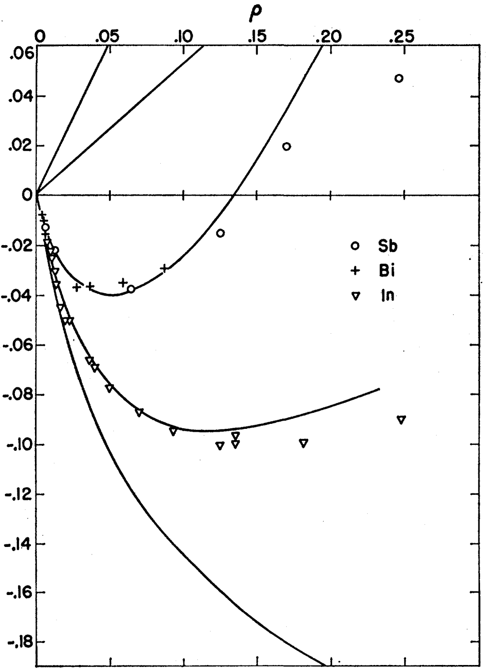

FIG. 10. Figure 1 replotted to exhibit the theory. The bottom curve represents the anisotropy effect taken from Fig. 3. The straight lines represent the linear "valence" effect. The sum of the two gives the theoretical fit for these tin systems. Comparing Figs. 10 and 1, we see that all but the highest $-\rho$ data are nicely fit.

different values of a is of no importance. The important thing is the region $l \sim \xi_0$. The point to be emphasized is that the present theory and the Seraphim empirical formula apply over a wide region extending from $l \gg \xi_0$ to $l \ll \xi_0$. For reference, values of ξ_0 appropriate to $a = 0.15$ are included in Table I.

V. CONCLUSIONS

The major conclusion of the present work is that measurements of the change in T_c with alloying may be fit quite well by a model in which this change is divided into two parts: a reduction of anisotropy due to scattering, and a linear effect upon the gross properties of the metal. For low doping, the former dominates; for higher doping, the latter does—three regions are separated at $l \sim \xi_0$. Over a large range, comprising both of these regions, the empirical formula of Seraphim *et al.* provides a good approximation to both theory and experiment.

We should, however, offer some words of warning to the reader. In the lowest region of measurable impurity density, the present theory is unreliable because it neglects lifetime effects caused by the electron-phonon interaction itself. What we are saying is that in the pure material there is a mechanism which has already smoothed out some of the anisotropy in the effective pairing interaction. Whenever the mean free path for impurity scattering is much smaller than the mean free path for phonon emission and absorption, the latter may safely be neglected. However, it should be included in a proper description of the purer specimens.[23]

The theory also begins to fail at the high-concentration end. Here the intrinsic properties of the metal may no longer be considered to depend linearly upon the density of impurities. Moreover, we begin to get overlap of impurity potentials so that the assumption of randomness, which permitted our calculation of the anisotropy effect, is no longer valid. These objections probably become serious above 10% of impurities.

However, the most limiting defect of the theory as it is presented here is the assumption that $\lambda^i = 1$ in the relationship (56) between χ and ρ. Because we feel that it lies at the core of future research on this subject, we wish to make clear once again the steps through which this assumption was reached. No assumption about λ^i is called for until one desires numbers for the "valence" and anisotropy parameters. Then (52) tells us that only the product $\lambda^i \langle a^2 \rangle$ can be determined. Moreover, since c_1^i [and hence, $(\partial T_c/\partial\rho)_0^i$ in (57)] will have an additional term proportional to $\ln\lambda^i$, it is clear that the "valence" parameter cannot be determined satisfactorily if the uncertainty in λ^i is excessive. Even if $\lambda^i \approx \lambda$, a constant, as it is for tin, only $\lambda\langle a^2 \rangle$ may be determined. If $\lambda = 2$ instead of our assumption of 1, it is easy to show, using Table I, that the new term in $\ln\lambda^i$ will be as large as the apparent value of the "valence" parameter itself.

It should be emphasized that the ratio of slopes for two systems with the same host is equal to the ratio of the pertinent λ^i's. That is, all of the difficulty which we have encountered above would disappear if just one λ^i were known for each host. It is not an assumption that $\lambda^i = \lambda$ for tin. The data tells us that this is true. The assumption consists of setting $\lambda = 1$. For In and Al this is not true. The reason is that some slopes for these hosts differ by a factor of 2. Therefore, we have actually made two assumptions for these metals: $\lambda^i = \lambda$ and $\lambda = 1$. For this reason, we feel that the main benefit of the numbers for In and Al are as an order-of-magnitude estimate of their parameters. On the other hand, we have quite a bit of confidence in our numbers for tin. We feel it would be somewhat unreasonable of nature to give us $\lambda^i = \lambda$ and $\lambda \neq 1$, for this would mean that eight impurities in tin possessed differential cross sections all deviating substantially from isotropy and all deviating in the same way. Table V displays values of ratios of λ^i for a number of impurities in tin, In, and Al.

TABLE V. Ratios of λ^i for a number of impurities in Sn, In, and Al. Values are quite imprecise due both to arbitrariness in placing empirical lines and to spread in data. However, Seraphim *et al.* and the authors agree on most values.

Impurities in Sn	in Al	in In
$\lambda(\mathrm{Pb}) \equiv 1$	$\lambda(\mathrm{Zn}) \equiv 1$	$\lambda(\mathrm{Sn}) \equiv 1$
$\lambda(\mathrm{Cd}) = 0.9$	$\lambda(\mathrm{Ag}) = 0.75$	$\lambda(\mathrm{Bi}) = 0.9$
$\lambda(\mathrm{Hg}) = 0.9$	$\lambda(\mathrm{Mg}) = 0.55$	$\lambda(\mathrm{Pb}) = 0.8$
$\lambda(\mathrm{In}) = 0.85$	$\lambda(\mathrm{Ge}) = 0.50$	$\lambda(\mathrm{Tl}) = 0.4$
$\lambda(\mathrm{Sb}) = 0.85$	$\lambda(\mathrm{Si}) = 0.50$	
$\lambda(\mathrm{Bi}) = 0.85$		

Finally, of course, we would like to compare our predictions for the tin parameters with measurements of those parameters. The only measurements we know of pertain to $\langle a^2 \rangle$. Recall that an immediate consequence of the separable pairing potential [Eq. (4)] in our model is that the anisotropy in the energy gap of the pure superconductor is also $a(\hat{\Omega})$. Thus, $\langle a^2 \rangle$ is the mean-squared anisotropy of the gap. Morse *et al.*[24] on the basis of ultrasonic attenuation measurements, have estimated the value of $\Delta(\hat{\Omega})$ in planes normal to three different directions in tin; Table VI shows that our value for $\langle a^2 \rangle$ is a reasonable one. Masuda[12] and Masuda and Redfield[13] have found that a similar value of $\langle a^2 \rangle$ will explain data on the nuclear spin-lattice relaxation time in superconducting Al. Moreover, Masuda has made the provocative discovery that a mean-free-path

---

[23] J. R. Schrieffer and co-workers have investigated lifetime contributions of this kind in pure superconductors and have found no substantial effects. Since our theory appears valid for a large region of τ when $\tau\Delta(0) \gg 1$, we have evidence that no substantial effects should be found.

[24] R. W. Morse *et al.* Ref. 9. See also table in E. A. Lynton, *Superconductivity* (Methuen and Company Ltd., London; John Wiley & Sons, Inc., New York, 1961), p. 130.

TABLE VI. Crystalline anisotropy of $\Delta(\Omega)$ for tin, taken from Morse *et al.* The values[a] of $2\Delta/kT_c$ pertain to a thin disk perpendicular to the direction of $\mathbf{q}\cdot\Delta$ is the gap at $T=0$.

Direction of $\mathbf{q}$	$2\Delta/kT_c$
Parallel to [001]	3.2 ± 0.1
Parallel to [110]	4.3 ± 0.2
Perpendicular to [001] and 18° from [100]	3.5 ± 0.1

[a] BCS gives $2\Delta/kT_c=3.5$ for isotropic weak-coupling superconductors.

effect contributes to the behavior of $\Delta(\hat{\Omega})$ in doped-Al. The present model is the groundwork for a quantitative investigation of this phenomenon.

ACKNOWLEDGMENTS

The authors are indebted to Professor J. R. Schrieffer for suggesting this problem and for his leadership during the preliminary stages of the work. We wish to thank Professor J. Bardeen, Professor D. Ginsberg, and J. D. Leslie for helpful discussions, and Dr. P. W. Anderson for useful comments.

APPENDIX: MORE EXACT DESCRIPTION OF ANISOTROPY EFFECT

In the body of the text, we wrote down a very approximate solution to the Eq. (36)

$$\Delta(\hat{\Omega},z)=-\frac{i}{z}\operatorname{sgn}[\operatorname{Im}(z)]\frac{n_I\bar{v}_F}{2}\int d\Omega'\frac{d\sigma}{d\Omega'}(\hat{\Omega}\rightarrow\hat{\Omega}')\times[\Delta(\hat{\Omega}',z)-\Delta(\hat{\Omega},z)]+[1+a(\hat{\Omega})]\epsilon_0. \quad \text{(A1)}$$

It is possible to solve this equation exactly when $d\sigma/d\Omega'$ and $a(\hat{\Omega})$ are known. This exact solution is not useful in the context of this paper because we do not know these functions, but the solution is given here for reference. We expand $d\sigma/d\Omega'$, a, and Δ in spherical harmonics as

$$a(\hat{\Omega})=\sum_{l,m}Y_{lm}(\theta,\varphi)a_{lm};$$
$$\Delta(\hat{\Omega},z)=\sum_{l,m}Y_{lm}(\theta,\varphi)\Delta_{l,m}(z); \quad \text{(A2)}$$
$$\frac{d\sigma}{d\Omega'}(\hat{\Omega}\rightarrow\hat{\Omega}')=\sum_{l,m}Y_{lm}(\theta,\varphi)\sigma_l Y_{lm}^*(\theta',\varphi').$$

From (A1)

$$\Delta_{0,0}=\epsilon_0,\quad l=0;$$

$$\Delta_{l,m}=-\frac{i}{z}\operatorname{sgn}[\operatorname{Im}(z)]\frac{n_I\bar{v}_F}{2}(\sigma_l-\sigma_0)\Delta_{l,m}+a_{lm}\epsilon_0,\quad l\neq0.$$

Hence,

$$\Delta_{l,m}=\frac{a_{lm}\epsilon_0}{1-(i/z)\operatorname{sgn}[\operatorname{Im}(z)](n_I\bar{v}_F/2)(\sigma_0-\sigma_l)},\quad l\neq0,$$

and

$$\Delta(\hat{\Omega},z)=\epsilon_0+\sum_{l,m}\frac{a_{lm}Y_{lm}(\theta,\varphi)\epsilon_0}{1-(i/z)\operatorname{sgn}[\operatorname{Im}(z)](n_I\bar{v}_F/2)(\sigma_0-\sigma_l)}. \quad \text{(A3)}$$

Then the gap equation reduces to

$$1=VN(0)\int_0^{\omega_D}\frac{d\omega}{\omega}\tanh\left(\frac{\beta\omega}{2}\right)\times\left\{1+\sum_{l,m}\frac{|a_{lm}|^2}{1+[(n_I\bar{v}_F/2\omega)(\sigma_0-\sigma_l)]^2}\right\}. \quad \text{(A4)}$$

It is natural to define

$$[\tau_l]^{-1}=n_I\bar{v}_F(\sigma_0-\sigma_l).$$

Then from (A4), it follows directly that the anisotropy produces a change in T_c

$$\frac{\delta T_c}{T_c}=-\sum_{l,m}|a_{lm}|^2 I_c\left(\frac{1}{kT_c\tau_l}\right). \quad \text{(A5)}$$

Notice that in the region in which

$$I_c(\chi)=k_1\chi+k_2\chi\ln\chi,$$

$$\frac{\delta T_c}{T_c}=-\sum_{l,m}|a_{lm}|^2\frac{1}{kT_c\tau_l}\left[k_1+k_2\ln\left(\frac{1}{kT_c\tau_l}\right)\right] \quad \text{(A6)}$$
$$=\sum_{l,m}|a_{lm}|^2\frac{0.078}{kT_c\tau_l}\ln(100kT_c\tau_l).$$

Since $1/\tau_l$ is proportional to the density of impurities, the empirical formula of Seraphim *et al.* is satisfied by this more exact solution.

In making correspondence with experiment, one should notice that σ_0 is the total impurity cross section and that the transport collision time is given by $\tau_{\text{tr}}=\tau_1$.